Prompt energization of relativistic and highly relativistic electrons during a substorm interval: Van Allen Probes observations

Citation: Foster, J. C., P. J. Erickson, D. N. Baker, S. G. Claudepierre, C. A. Kletzing, W. Kurth, G. D. Reeves, et al. "Prompt Energization of Relativistic and Highly Relativistic Electrons During a Substorm Interval: Van Allen Probes Observations." Geophysical Research Letters 41, no. 1 (January 15, 2014): 20–25.

As Published: http://dx.doi.org/10.1002/2013GL058438

Publisher: American Geophysical Union (AGU)

Persistent URL: http://hdl.handle.net/1721.1/109288

Version: Final published version: final published article, as it appeared in a journal, conference proceedings, or other formally published context

AGU PUBLICATIONS

Geophysical Research Letters

RESEARCH LETTER
10.1002/2013GL058438

Special Section:
Early Results from the Van Allen Probes(Closed to new submissions Nov 1, 2013)

Key Points:
- Substorm dynamics are important for highly relativistic electron energization
- Cold plasma preconditioning is significant for rapid relativistic energization
- Relativistic / highly relativistic electron energization can occur in < 5 hrs

Correspondence to:
P. J. Erickson,
pje@haystack.mit.edu

Citation:
Foster, J. C., et al. (2014), Prompt energization of relativistic and highly relativistic electrons during a substorm interval: Van Allen Probes observations, *Geophys. Res. Lett.*, *41*, 20–25, doi:10.1002/2013GL058438.

Received 23 OCT 2013
Accepted 16 DEC 2013
Accepted article online 19 DEC 2013
Published online 15 JAN 2014

Prompt energization of relativistic and highly relativistic electrons during a substorm interval: Van Allen Probes observations

J. C. Foster[1], P. J. Erickson[1], D. N. Baker[2], S. G. Claudepierre[3], C. A. Kletzing[4], W. Kurth[4], G. D. Reeves[5], S. A. Thaller[6], H. E. Spence[7], Y. Y. Shprits[8], and J. R. Wygant[6]

[1]Atmospheric Sciences Group, Haystack Observatory, Massachusetts Institute of Technology, Westford, Massachusetts, USA, [2]Laboratory for Atmospheric and Space Physics, University of Colorado, Boulder, Colorado, USA, [3]Space Sciences Department, The Aerospace Corporation, Los Angeles, California, USA, [4]Department of Physics and Astronomy, University of Iowa, Iowa City, Iowa, USA, [5]Los Alamos National Laboratory, Los Alamos, New Mexico, USA, [6]Department of Physics and Astronomy, University of Minnesota, Minneapolis, Minnesota, USA, [7]Institute for Study of Earth, Oceans, and Space, University of New Hampshire, Durham, New Hampshire, USA, [8]Institute of Geophysics and Planetary Physics, University of California, Los Angeles, California, USA

Abstract On 17 March 2013, a large magnetic storm significantly depleted the multi-MeV radiation belt. We present multi-instrument observations from the Van Allen Probes spacecraft Radiation Belt Storm Probe A and Radiation Belt Storm Probe B at ~6 *Re* in the midnight sector magnetosphere and from ground-based ionospheric sensors during a substorm dipolarization followed by rapid reenergization of multi-MeV electrons. A 50% increase in magnetic field magnitude occurred simultaneously with dramatic increases in 100 keV electron fluxes and a 100 times increase in VLF wave intensity. The 100 keV electrons and intense VLF waves provide a seed population and energy source for subsequent radiation belt enhancements. Highly relativistic (>2 MeV) electron fluxes increased immediately at L* ~ 4.5 and 4.5 MeV flux increased >90 times at L* = 4 over 5 h. Although plasmasphere expansion brings the enhanced radiation belt multi-MeV fluxes inside the plasmasphere several hours postsubstorm, we localize their prompt reenergization during the event to regions outside the plasmasphere.

1. Introduction

A large geomagnetic disturbance on 17 March 2013 (minimum *Dst* ~ −130 nT) produced a sharp depletion of Earth's energetic electron radiation belts reaching in to L ~ 3 *Re*, followed by a prompt reenergization and recovery of electrons at multi-MeV energies early on 18 March. *Baker et al*. (this issue) describe this event and place it into context within the overall evolution of radiation belts observed by the relativistic electron-proton telescope (REPT) [*Baker et al*., 2012] during the first year of operations of the Van Allen Probes spacecraft, referred to here as Radiation Belt Storm Probes (RBSP) A and B. A focus of the Van Allen Probes mission is the investigation of processes leading to loss and energization in the radiation belts [*Mauk et al*., 2012]. The mechanisms involved in the energization of multi-MeV electrons over only a few hours, as observed in the 17 March event, are largely unknown. *Shprits et al*. [2008] describe some of the ongoing research in this area. Without the support of sufficient observations, it is difficult to understand the means by which energy propagates through the spectrum all the way to the multi-MeV tail of the energy distribution function. Here we investigate the role of substorm processes in providing conditions favorable to such rapid reenergization.

2. Observations

We present detailed multi-instrument observations of ionosphere and magnetosphere conditions during a substorm event that occurred late on 17 March 2013, while both RBSP spacecraft were near apogee in the midnight sector. Earlier on that day, shortly after 20 UT, RBSP-A exited the plasmasphere, near 20 magnetic local time (MLT), crossing the high-altitude region of rapid sunward flow and plasmasphere erosion associated in the ionosphere with the subauroral polarization stream [*Foster and Vo*, 2002].

Figure 1 presents a snapshot of north polar region electron density content below ~4 *Re* from GPS total electron content (TEC) data at 21:45 UT (noon at the top, polar MLT—invariant latitude coordinates). The markings on the

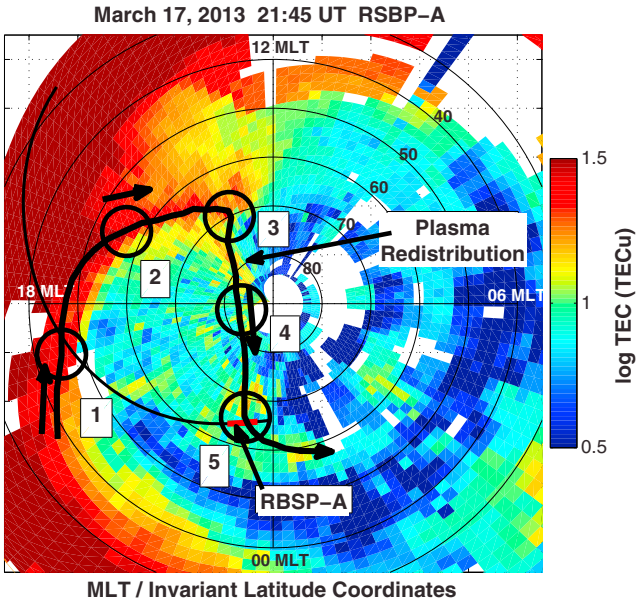

Figure 1. Snapshot of north polar region electron density content below ~4 *Re* from GPS total electron content data at 21:45 UT (noon at the top, polar MLT—invariant latitude coordinates). The five regions involved in cold plasma redistribution in this event are marked on the figure (see text). The ionospheric projection of the orbital position of RBSP-A during the substorm event is shown in red in region 5.

figure indicate the five regions involved in cold plasma redistribution in this event. Using a combination of Van Allen Probes data, ground-based radar, and DMSP observations, *Foster et al.* (this issue) interrelate low-altitude and GPS TEC measurements with in situ plasmaspheric characteristics. They describe the redistribution fluxes of plasmasphere and ionosphere material from dusk sector field lines at the plasmapause (1) to the dayside cusp (3) via the storm enhanced density [*Foster*, 1993; *Foster et al.*, 2002]/plasmasphere erosion plume (2), and back across polar latitudes to the midnight sector (4) in a polar tongue of ionization (TOI) [*Foster et al.*, 2005]. *Foster et al.* (this issue) report a pronounced increase in polar cap TEC magnitude beginning at the onset of the 17 March storm and continuing sporadically until ~22 UT, at which time a sudden decrease in north polar TOI was observed. Relevant for this study, antisunward flow in the TOI carries the eroded material into the midnight auroral oval (region 5) along field lines involved in nightside reconnection and particle energization.

The near-equatorial (inclination ~10°), highly elliptical orbits of the two RBSP spacecrafts have trajectories moving from the inner plasmasphere to L ~ 6 with an ~9 h orbital period. Later on 17 March, RBSP-B preceded RBSP-A by ~1 h, with an apogee on field lines mapping down to the region where TOI plasma was exiting the polar cap at midnight, as seen in GPS TEC measurements. The orbital position of RBSP-A between 21 UT and 22 UT on 17 March, mapped onto the underlying ionosphere, is shown in red in region 5 in Figure 1.

In Figure 2, we present high-altitude ($R > 5$ *Re*) midnight sector observations of patchy cold plasma density enhancements as observed by both RBSP-A (Figure 2a) and RBSP-B (Figure 2c). Electron density was determined both from electric and magnetic field instrument suite and integrated science (EMFISIS) (blue) plasma wave and magnetometer observations [*Kletzing et al.*, 2012] and from electric field and waves (EFW) [*Wygant et al.*, 2013] probe potentials (red). Near apogee, the EFW density measuring technique becomes invalid due to spacecraft eclipse effects. The patches of high-altitude TOI material show enhanced densities of 20 to 40 cm^{-3}. Similar to the ground-based TOI temporal behavior, cold plasma density encountered by both spacecraft was sharply reduced on the high-altitude field lines after ~22 UT.

Figure 2b displays the magnetic field magnitude observed at RBSP-A by the EMFISIS magnetometer. A pronounced decrease in |B| (field stretching) was seen shortly after 22:00 UT, followed by a 50% increase (dipolarization) at ~22:17 UT. These effects are signatures of a substorm-like reconfiguration of the nightside magnetic field. (Although not shown here, the dipolarization signature observed at RBSP-B was nearly simultaneous, occurring ~2 min earlier than shown for RBSP-A. Throughout the paper, we refer event timing to 22:17 UT, the approximate time of the substorm dipolarization as observed at RBSP-A.) Accompanying the dipolarization, Scandinavian riometer stations

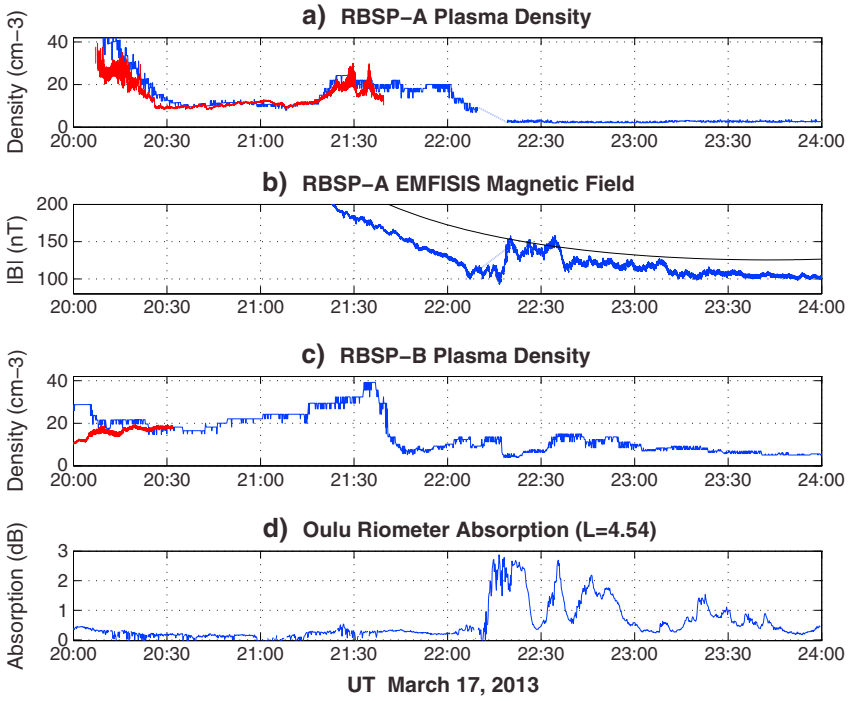

Figure 2. (a) In situ determination of midnight sector cold plasma density at the ~5 *Re* altitude of RBSP-A was determined both from EMFISIS (blue) plasma wave and magnetometer observations and from EFW electric field probe potentials (red). (b) RBSP-A EMFISIS magnetometer observation of the magnetic field dipolarization (substorm) with onset at ~22:17 UT. Modeled variation of equatorial |B| is shown in black. (c) RBSP-B cold plasma density determinations (same format as Figure 2a). (d) Riometer absorption measured at Oulu, Finland, very near the ground track of the RBSP spacecraft at the time of the substorm event indicates the onset of ~50 keV electron precipitation during the 20:17 UT event.

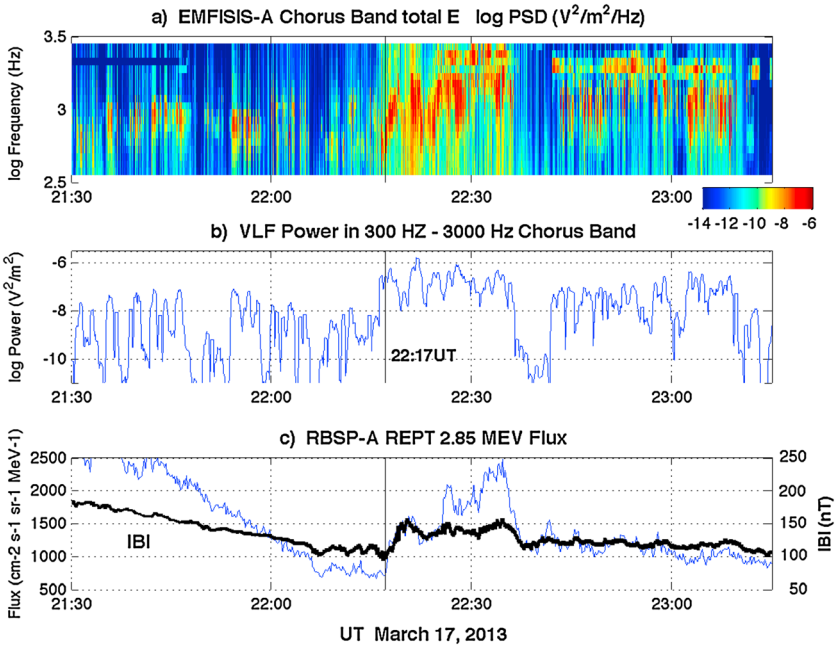

Figure 3. (a) Total electric field power spectral density at VLF chorus band frequencies as observed with the EMFISIS instrument on RBSP-A. (b) Total chorus band wave power between 300 Hz and 3000 Hz. (c) EMFISIS magnetic field magnitude (heavy curve) overplotted on REPT-A 2.85 MeV electron flux observations (blue curve).

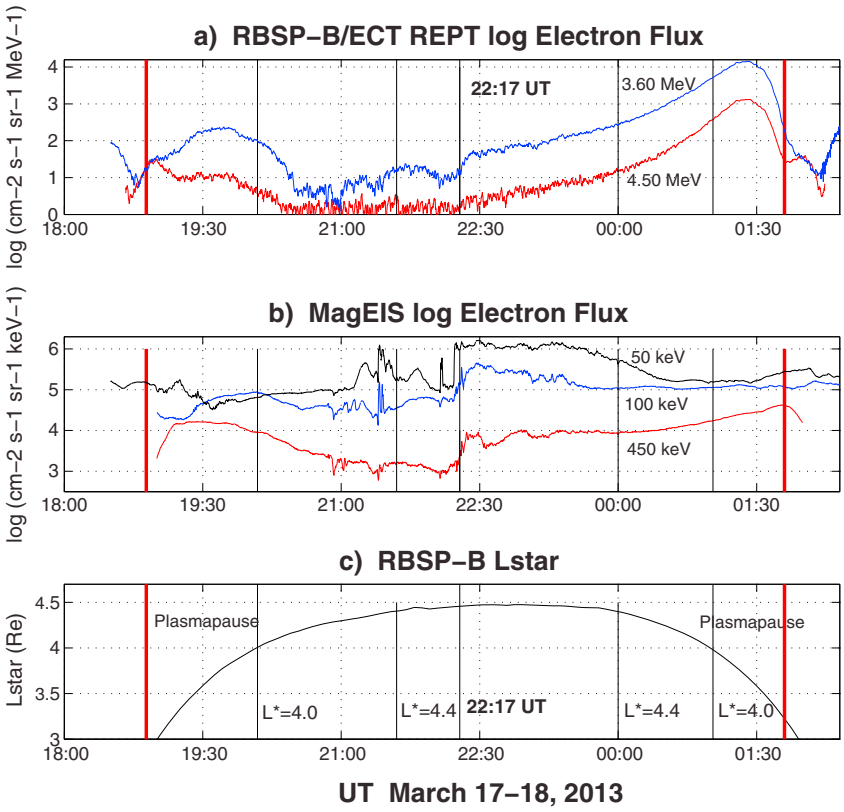

Figure 4. (a) REPT-B 3.60 MeV (blue) and 4.50 MeV (red) highly relativistic electron flux observations show a prompt enhancement at the time of the 22:17 UT substorm and (with respect to the outbound pass) significant enhancement of fluxes during the subsequent inbound pass between L* ~ 4.5 and L* ~ 3.5. (b) MagEIS-B energetic (50 keV and 100 keV) and near-relativistic (450 keV) electron flux observations. (c) L* calculated for the outbound/inbound pass of RBSP-B indicates that the spacecraft observations near apogee were made at near-constant L* ~ 4.5 *Re* during an ~4 h interval centered on the substorm onset. Red fiducial lines indicate the observed 30 cm^{-3} plasmapause locations, and times of electron flux observations at L* = 4.0 *Re* and L* = 4.4 *Re* are indicated.

very near the ground magnetic projection of the RBSP orbital positions observed a rapid onset of midnight sector absorption, indicating energetic (>50 keV) electric precipitation. Absorption was strongest and began earliest at the Oulu, Finland site (Figure 2d) at L ~ 4.54, with absorption onset several minutes later at higher latitude stations.

The RBSP plasma density data in Figure 2 are the first published observations of TOI plasma near the apex of nightside field lines. The long duration of the TOI fluxes during the 17 March 2013 event reported by *Foster et al*. (this issue) suggests that high-latitude nightside magnetospheric field lines were richly populated with plasmaspheric material prior to the 22:17 UT dipolarization and electron injection (cf. Figure. 4) event.

In Figure 3a, we present the total electric field power spectral density (PSD) at VLF chorus band frequencies as observed with the EMFISIS instrument on RBSP-A. Total VLF chorus band power, defined as the integral of the PSD observations between 300 Hz and 3000 Hz (Figure 3b), increases by a factor of 100 associated with the 22:17 UT onset of the magnetic field dipolarization. Much of the emission in this VLF band is "hiss-like," but there are times when discrete risers are clearly present. EMFISIS magnetic field magnitude is repeated as the heavy curve in Figure 3c overplotted on REPT-A 2.85 MeV electron flux observations (blue curve). Between 22:15 and 22:35 UT, the ambient magnetic field strength increased by 50% and chorus band intensity increased by ~100 times, with center frequency rising to ~2000 Hz. The inferred ambient cold plasma density was low at ~2 cm^{-3} (cf. Figure 2), and the observed flux of highly relativistic 2.85 MeV electrons increased by a factor of ~3 in ~5 min in association with increases in |B| during the depolarization event. VLF wave frequency, intensity, and 2.85 MeV electron flux increased synchronously with the magnetic field variations.

RBSP-B, approaching apogee at the time of the 22:17 UT substorm onset, also observed prompt increases in both relativistic (> ~ 500 keV) and highly relativistic (>2 MeV) electrons. In Figure 4, we present electron flux observations

measured by the REPT and magnetic electron ion spectrometer (MagEIS) [*Blake et al*., 2012] instruments, both from the RBSP-B energetic particle, composition, and thermal plasma (ECT) instrument suite [*Spence et al*., 2013]. These clearly indicate the timing and extent of electron energization associated with the substorm onset. Figure 4a plots the log electron flux from REPT as a function of UT for two selected highly relativistic energy channels at 3.60 MeV (blue curve) and 4.50 MeV (red curve), while Figure 4b shows the log electron flux from MagEIS for enegetic 50 keV (black) and 100 keV (blue) and relativistic 450 keV (red curve) electrons. The spacecraft L* coordinates are shown in Figure 4c (bottom), calculated using the Tsyganenko 2004 dynamic model [*Tsyganenko and Sitnov*, 2005]. (L* [*Roederer*, 1970] is directly proportional to the integral of the magnetic flux contained within the surface defined by a charged particle moving in the Earth's geomagnetic field (B). Under adiabatic changes to B, L* is a conserved quantity.) Fiducial lines indicate plasmapause positions (red, Ne = 30 cm^{-3}) as estimated by the EFW instrument, the substorm onset time at 22:17 UT, and the times of spacecraft passage through L* = 4.0 and L* = 4.4 before and after the large magnetic reconfiguration. At the time of the substorm, both RBSP-A and RBSP-B observed prompt increases in the MeV electron fluxes and then observed nearly identical Lstar profiles after ~22:35 UT.

The electron flux behavior is striking in its large increases over short intervals. In an ~5 h separation between L* = 4.0 crossings, 3.60 MeV highly relativistic electron fluxes increased by a factor of 56, while 4.50 MeV flux increased by an even larger factor of 95. For an earlier event, *Reeves et al*. [2013] examined RBSP measurements of phase space density profiles to show signatures of local acceleration of highly relativistic electrons in the heart of the radiation belts centered near L* ~ 4. At lower energies, 100 keV fluxes increased between visits to the L* = 4.0 region by 1.5 times and 450 keV fluxes increased by more than 2 times.

The behavior of energetic (100 keV) electrons is fundamentally different from highly energetic electrons after substorm onset. In particular, RBSP-B remains at a nearly constant L* = 4.5 for several hours postsubstorm, and during this interval, 100 keV electron levels quickly become relatively constant while 2.85 MeV energies and higher show steady, large increases in flux levels. The 450 keV electron fluxes exhibit an intermediate response between these two populations, starting with a relatively constant postsubstorm flux level but rising steadily in the early UT hours of 18 March.

3. Discussion

Energetic electrons at 50–100 s of keV are still responsive to convection electric fields and can be injected inward to the plasmapause, providing free energy for chorus waves [e.g., *Foster and Rosenberg*, 1976] that can subsequently help to accelerate a seed population of 100 s of keV electrons up to MeV energies. In particular, *Baker et al*. [1982] report modeling results showing that to get deep injections of energetic particles into the inner magnetosphere, one needs to have a localized "wedge" region of strong inductive electric fields (they presumed the substorm current wedge region). Such fields allow very energetic particles to penetrate inward rapidly enough to avoid the effects of gradient-curvature drift forces. The medium energy electrons up to a few hundred keV are a key output of the substorm acceleration and transport process. They are a power law "tail" component of the electron flux distribution that can be affected simultaneously by convective and diffusive processes. They form the seed population that is essential for the ultimate radiation belt enhancements. Electrons with relativistic energies $>$500 keV are mostly gradient and curvature drifting and convection cannot inject them far inward [e.g., *Liu et al*., 2003]. Another difference is that above a few MeV, electrons are not effectively scattered by whistler mode chorus, and thus, quasi-linear diffusive local acceleration by chorus band waves is not likely to be efficient.

Cold plasma density plays an important role in the reenergization of the MeV electron radiation belts that were severely depleted early in the 17 March storm and in their subsequent long lifetime in the inner magnetosphere. *Baker et al*. (this issue) stress this point, concluding that relativistic electron acceleration occurs when the outer zone is situated well outside the plasmasphere, providing an opportunity for interactions between chorus mode waves lying beyond the plasmapause and the substorm-generated "seed" particles [see *Baker and Kanekal*, 2008] necessary for relativistic electron production. The Van Allen Probes observations we present here indicate that the 17 March 22:17 UT substorm was accompanied by ample magnetospheric fluxes of the energetic ring current and relativistic (50 keV–500 keV) electrons, potentially serving as seed particles for energization to multi-MeV energies. *Boyd et al*. (this issue) explore the phase space density time dependence of the electron seed population for this event. Cyclotron resonance interactions with tens of keV injected electrons can amplify chorus band

whistler mode waves, matching the observations shown in Figure 3 and resulting in the energetic electron precipitation inferred from the midnight sector riometer observations shown in Figure 2.

This scenario is further supported by plasmapause dynamics during the event. Heavy red fiducial lines on Figure 4 mark the position of the plasmapause ($Ne = 30\,cm^{-3}$) observed on the RBSP-B outbound and inbound crossings bracketing the substorm. The plasmapause was observed at $L^* \sim 3$ at the time of the substorm, and the subsequent prompt energization shown in Figure 4a was observed outside the plasmasphere between L^* values of 3.5 and 4.5.

Furthermore, plasmasphere refilling later on 18 March caused the $Ne = 30\,cm^{-3}$ plasmapause location to expand continually, reaching $L^* \sim 3.8$ by 05 UT and $L^* \sim 4.0$ by 10 UT. This expansion places the peak of the multi-MeV particles, now recovered in flux levels, inside the plasmasphere. *Shprits et al.* [2013] model a similar situation in which electrons at low L shells find themselves inside the plasmasphere in a very different plasma environment, where electromagnetic ion cyclotron waves are not present and the strongest emissions are whistler mode hiss. That study points out that, in this configuration, energetic and relativistic electrons will resonate with hiss waves near the equator and will be lost to the atmosphere on a time scale of a few days. However, highly relativistic electrons will be out of resonance with hiss waves near the equator, providing the reason why the unusual storage ring of highly relativistic electrons reported by *Baker et al.* [2013] can persist for over four weeks.

The 17 March multipoint observations presented here indicate the significant role that substorm processes can play in creating a seed population of 100 keV electrons and VLF wave enhancements that can lead to a prompt energization of relativistic and highly relativistic electrons in the region outside the plasmapause.

Acknowledgments

We thank J. Vierinen for help in obtaining the Scandinavian sector riometer data and A. Jaynes and M. Henderson for making REPT L* and phase space density data available to assist in this study. Work at MIT Haystack Observatory was supported by a Van Allen Probes subaward from the University of Minnesota to the Massachusetts Institute of Technology. Work at the University of Colorado and University of New Hampshire was supported by RBSP-ECT funding provided by JHU/APL contract 967399 under NASA's Prime contract NAS5-01072. Y.Y.S. acknowledges support from NASA NNX10AK99G, NNX13AE34G, NNX09AF51G, and NSF AGS-1203747 grants. All Van Allen Probes data used are publicly available at www.rbsp-ect.lanl.gov.

The Editor thanks Andrei Demekhov and an anonymous reviewer for their assistance in evaluating this paper.

References

Baker, D. N., and S. G. Kanekal (2008), Solar cycle changes, geomagnetic variations, and energetic particle properties in the inner magnetosphere, *J. Atmos. Sol. Terr. Phys.*, *70*, 195–206.

Baker, D. N., et al. (1982), Observation and Modeling of Energetic Particles at Synchronous Orbit on July 29, 1977, *J. Geophys. Res.*, *87*, 5917–5932, doi:10.1029/JA087iA08p05917.

Baker, D. N., et al. (2012), The Relativistic Electron-Proton Telescope (REPT) instrument on board the Radiation Belt Storm Probes (RBSP) spacecraft: Characterization of Earth's radiation belt high-energy particle populations, *Space Sci. Rev.*, *179*, 337–381, doi:10.1007/s11214-012-9950-9.

Baker, D. N., et al. (2013), A long-lived relativistic electron storage ring embedded in Earth's outer Van Allen belt, *Science*, *340*, 186–190, doi:10.1126/science.1233518.

Blake, J. B., et al. (2012), Magnetic Electron Ion Spectrometer (MagEIS) instruments aboard the Radiation Belt Storm Probes (RBSP) spacecraft, *Space Sci. Rev.*, *179*, 383–421, doi:10.1007/s11214-013-9991-8.

Foster, J. C. (1993), Storm-time plasma transport at middle and high latitudes, *J. Geophys. Res.*, *98*, 1675–1689.

Foster, J. C., and T. J. Rosenberg (1976), Electron precipitation and VLF emissions associated with cyclotron resonance interactions near the plasmapause, *J. Geophys. Res.*, *81*, 2183–2192.

Foster, J. C., and H. B. Vo (2002), Average characteristics and activity dependence of the subauroral polarization stream, *J. Geophys. Res.*, *107*(A12), 1475, doi:10.1029/2002JA009409.

Foster, J. C., P. J. Erickson, A. J. Coster, J. Goldstein, and F. J. Rich (2002), Ionospheric signatures of plasmaspheric tails, *Geophys. Res. Lett.*, *29*(13), 1623, doi:10.1029/2002GL015067.

Foster, J. C., et al. (2005), Multiradar observations of the polar tongue of ionization, *J. Geophys. Res.*, *110*, A09S31, doi:10.1029/2004JA010928.

Kletzing, C. A., et al. (2012), The Electric and Magnetic Field Instrument and Integrated Science (EMFISIS) on RBSP, *Space Sci. Rev.*, doi:10.1007/s11214-013-9993-6.

Liu, S., M. W. Chen, L. R. Lyons, H. Korth, J. M. Albert, J. L. Roeder, and P. C. Anderson (2003), Contribution of convective transport to stormtime ring current electron injection, *J. Geophys. Res.*, *107*(A10), 1372, doi:10.1029/2003JA010004.

Mauk, B. H., N. J. Fox, S. G. Kanekal, R. L. Kessel, D. G. Sibeck, and A. Ukhorskiy (2012), Science objectives and rationale for the Radiation Belt Storm Probes mission, *Space Sci. Rev.*, doi:10.1007/s11214-012-9908-y.

Reeves, G. D., et al. (2013), Electron acceleration in the heart of the Van Allen radiation belts, *Science*, *341*, 991–994, doi:10.1126/science.1237743.

Roederer, J. G. (1970), *Dynamics of Geomagnetically Trapped Radiation*, Springer-Verlag, New York.

Shprits, Y. Y., D. A. Subbotin, N. P. Meredith, and S. R. Elkington (2008), Review of modeling of losses and sources of relativistic electrons in the outer radiation belts: II. Local acceleration and loss, *J. Atmos. Sol. Terr. Phys.*, *70*(14), 1694–1713, doi:10.1016/j.jastp.2008.06.014.

Shprits, Y. Y., D. Subbotin, A. Drozdov, M. E. Usanova, A. Kellerman, K. Orlova, D. N. Baker, D. L. Turner, and K.-C. Kim (2013), Unsual stable trapping of the ultrarelativistic electrons in the Van Allen radiation belts, *Nat. Phys.*, *9*, 699–703, doi:10.1038/NPHYS2760.

Spence, H. E., et al. (2013), Science goals and overview of the Radiation Belt Storm Probes (RBSP) Energetic Particle, Composition, and Thermal Plasma (ECT) Suite on NASA's Van Allen Probes Mission, *Space Sci. Rev.*, *179*, 311–336, doi:10.1007/s11214-013-0007-5.

Tsyganenko, N. A., and M. I. Sitnov (2005), Modeling the dynamics of the inner magnetosphere during strong geomagnetic storms, *J. Geophys. Res.*, *110*, A03208, doi:10.1029/2004JA010798.

Wygant, J. R., et al. (2013), The Electric Field and Waves (EFW) instruments on the Radiation Belt Storm Probes Mission, *Space Sci. Rev.*, *179*, 183–220, doi:10.1007/s11214-013-0013-7.